



Suppressed superexchange interactions in the cuprates by bond-stretching oxygen phononsShaozhi Li ^{*}*Materials Science and Technology Division, Oak Ridge National Laboratory, Oak Ridge, Tennessee 37831, USA
and Department of Physics and Astronomy, Clemson University, Clemson, South Carolina 29631, USA*Steven Johnston *Department of Physics and Astronomy, and Institute for Advanced Materials and Manufacturing, The University of Tennessee, Knoxville,
Tennessee 37996, USA* (Received 24 May 2022; revised 19 May 2023; accepted 31 October 2023; published 14 November 2023)

We study a multiorbital Hubbard–Su-Schrieffer-Heeger model for the one-dimensional (1D) corner-shared cuprates in the adiabatic and nonadiabatic limits using exact diagonalization and determinant quantum Monte Carlo. At half filling and in the adiabatic limit, lattice dimerization can be achieved only over a narrow range of couplings slightly below a critical coupling g_c . Beyond this value, the sign of the effective hopping changes, and the lattice becomes unstable. Strong lattice fluctuations replace the dimerization state in the nonadiabatic case. We also examine the model’s temperature-dependent uniform and dynamical magnetic susceptibilities and compare them to the results of an effective spin-1/2 Heisenberg model. In doing so, we demonstrate that lattice fluctuations induced by the e -ph interaction suppress the effective superexchange interaction when $g < g_c$. Our results elucidate the effect of bond-stretching phonons in the parent cuprate compounds in general and are particularly relevant to 1D cuprates, where strong e -ph interactions have recently been inferred.

DOI: [10.1103/PhysRevB.108.L201113](https://doi.org/10.1103/PhysRevB.108.L201113)

Introduction. There is growing experimental evidence that the electron-phonon (e -ph) or the spin-phonon interaction plays a crucial role in shaping the magnetic properties of correlated materials such as the high-temperature cuprate superconductors [1–9], the Kitaev spin-liquid candidate α - RuCl_3 [10–13], and multiferroics [14–16]. Nevertheless, understanding the physics of strong e -ph interactions in correlated quantum materials remains a significant challenge for the community.

Atomic motion in correlated materials can couple to charge carriers via several mechanisms. For example, variations in the interatomic distances naturally modulate the nearest-neighbor hopping integrals. This mechanism can be described using a Su-Schrieffer-Heeger (SSH)-like e -ph interaction, which is off diagonal in orbital space [17–21]. Conversely, changes in the local bond distances can modify local Madelung energies [22,23]. This effect can be captured using a(n) (orbital) diagonal Holstein-like interaction, where the atomic displacements couple directly to the on-site orbital energies. In the context of strongly correlated models, the diagonal e -ph interaction has received far more attention. For example, numerous studies of the Hubbard-Holstein model and its extensions have been carried with a variety of nonperturbative numerical methods [24–40]. Comparatively fewer nonperturbative studies have been conducted for correlated SSH models [41–48], and nearly all of these have focused on single-band models.

In this Letter, we use the one-dimensional (1D) corner-shared cuprates as a platform to study the effects of the

transition-metal (TM)-O bond-stretching modes in oxides. Our focus on the 1D cuprates is partly motivated by recent experiments that have inferred strong coupling to optical oxygen phonons in the spin-chain material $\text{Ba}_{2-x}\text{Sr}_x\text{CuO}_{3+\delta}$ [49,50]. However, we also wish to understand better the 2D high-temperature superconducting cuprates, where numerous experiments have suggested a strong coupling to the optical Cu-O bond-stretching modes [1–9], leading to a sizable modulation of Cu-O hopping integral t_{pd} [23]. More specifically, we study a multiorbital Hubbard-SSH model for corner-shared cuprate spin chains, which retains the full Cu and O orbital basis and the optical Cu-O bond-stretching modes. The model is solved using exact diagonalization (ED) and determinant quantum Monte Carlo (DQMC), which provide numerically exact results on finite-size clusters. (Here, we can run DQMC simulations at comparatively low temperatures due to a milder sign problem in 1D [51–53].)

Focusing on half filling, we find that the system has a narrow window of coupling strengths $g \lesssim g_c$ where it supports a strong $q = \pi/a$ bond correlations. (In the adiabatic limit, the lattice is fully dimerized; in the antiadiabatic limit, the bonds are strongly fluctuating at the lowest accessible temperatures.) Above this window, the lattice becomes unstable due to an unphysical sign change in the effective hopping integrals. Below this window, strong antiferromagnetic (AFM) correlations persist, but the SSH interaction suppresses the overall magnitude of the superexchange interaction. This result is in direct contrast to the predictions of the single-band Hubbard-Holstein model, where weak e -ph interactions can enhance J by lowering the effective Coulomb interaction U . Our results imply that the bond-stretching motion of the O atoms can directly affect the cuprate’s magnetism, as proposed

^{*}lishaozhiphys@gmail.com

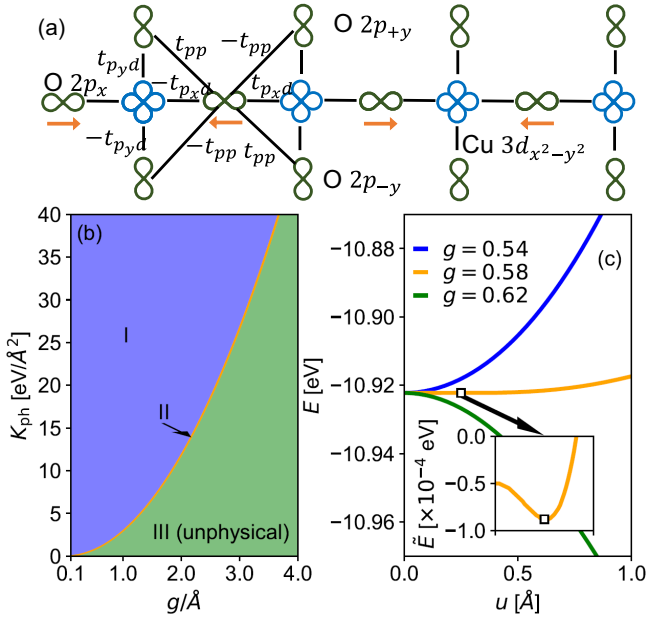


FIG. 1. The four-orbital SSH-Hubbard model. (a) A sketch of the four-orbital CuO pd model describing the corner-shared spin-chain cuprates such as Sr_2CuO_3 . The orange arrow denotes the motion of oxygen atoms for the half-breathing mode. (b) The phase diagram of the four-orbital SSH-Hubbard model in the e -ph coupling g and elastic constant K_{ph} plane in the adiabatic limit. (c) The variation of energy as a function of the displacement u for three different values of g at $K_{\text{ph}} = 1 \text{ eV}/\text{\AA}^2$.

in Ref. [54]. The physical principles we identify here are expected to be general and should carry over to models for the two-dimensional cuprates.

Model. We consider a four-orbital Hubbard-SSH model for the corner-shared cuprates, which includes the Cu $3d_{x^2-y^2}$ and O $2p_{x/y}$ orbitals (the pd model hereafter), as shown in Fig. 1(a). Its Hamiltonian is given by

$$\begin{aligned}
 H = & (\epsilon_d - \mu) \sum_{i,\sigma} \hat{n}_{i,\sigma}^d + \sum_{j,\gamma,\sigma} (\epsilon_{p,\gamma} - \mu) \hat{n}_{j,\gamma,\sigma}^p \\
 & + \sum_{\substack{\langle i,j \rangle \\ \gamma,\sigma}} t_{p\gamma d}^{ij} (d_{i,\sigma}^\dagger p_{j,\gamma,\sigma} + \text{H.c.}) + \sum_{\substack{\langle j,j' \rangle \\ \gamma,\gamma',\sigma}} t_{p\gamma p\gamma'}^{jj'} p_{j,\gamma,\sigma}^\dagger p_{j',\gamma',\sigma} \\
 & + U_d \sum_i \hat{n}_{i,\uparrow}^d \hat{n}_{i,\downarrow}^d + U_p \sum_{j,\gamma} \hat{n}_{j,\gamma,\uparrow}^p \hat{n}_{j,\gamma,\downarrow}^p \\
 & + \sum_j \left(\frac{\hat{p}_j^2}{2M} + K_{\text{ph}} \hat{x}_j^2 \right). \quad (1)
 \end{aligned}$$

Here, $\langle \dots \rangle$ denotes a sum over nearest-neighbor orbitals; $d_{i,\sigma}^\dagger$ and $p_{j,\gamma,\sigma}^\dagger$ create a hole with spin σ ($=\uparrow, \downarrow$) on the i th Cu $3d_{x^2-y^2}$ and the j th O $2p_\gamma$ ($\gamma = x, \pm y$) orbitals, respectively; ϵ_d and $\epsilon_{p,\gamma}$ are the on-site energies; $\hat{n}_{i,\sigma}^d$ and $\hat{n}_{j,\gamma,\sigma}^p$ are the number operators for the $3d_{x^2-y^2}$ and $2p_\gamma$ orbitals, respectively; \hat{x}_j and \hat{p}_j are the displacement and momentum operators for the $2p_x$ orbital; g is the e -ph coupling strength; and $t_{p\gamma d}^{ij}$ and $t_{p\gamma p\gamma'}^{jj'}$ are the nearest-neighbor Cu-O ($2p_\gamma$) and O-O hopping integrals. Their signs are shown in Fig. 1(a).

We assume that the vibration of the oxygen atom linearly modulates the magnitude of the hopping $t_{p\gamma d}^{ij}(x_j) = t_{p\gamma d}^{ij}(1 - Q_\pm g \hat{x}_j)$, where $Q_\pm = \pm 1$ for hopping to the left/right. The effective hopping integrals will retain the phase convention shown in Fig. 1(a) provided that the magnitude of the displacements is not too large. U_d and U_p are the on-site Hubbard interactions on the Cu and O orbitals; μ is the chemical potential, which sets the average hole density. M and K_{ph} are the mass and elastic constant, and the phonon frequency is given by $\omega_{\text{ph}} = \sqrt{\frac{2K_{\text{ph}}}{M}}$. Throughout this work, we study the model at half filling (1 hole/unit cell) and set (in units of eV) $\epsilon_d = 0$, $\epsilon_{p,x} = 3$, $\epsilon_{p,y} = 3.5$, $|t_{p_x d}| = 1.5$, $|t_{p_y d}| = 1.8$, $|t_{pp}| = 0.75$, $U_d = 8$, $U_p = 4$. These parameters are inferred from prior experimental and theoretical work (see Ref. [52]). Periodic boundary conditions are assumed.

Our model includes the motion of $2p_x$ orbitals, which is more critical for describing the electronic structure along the chain direction. One should also consider the movement of the $2p_y$ orbital when modeling a 2D system.

Adiabatic limit. We first examine the adiabatic limit $\omega_{\text{ph}} \rightarrow 0$, where phonons can be treated as classical fields. In this case, we consider the half-breathing mode and parametrize $x_j = (-1)^j u$. We then obtain the ground state by minimizing the system's energy $E(u)$ with respect to u , which is done by performing ED on a Cu_4O_{12} cluster. Figure 1(b) plots the resulting $K_{\text{ph}}-g$ phase diagram, where we find three distinct solutions (denoted as I, II, and III), each characterized by their $E(u)$ behavior [see Fig. 1(c)]. In region I, the chain has strong antiferromagnetic correlations, and $E(u)$ is a monotonically increasing function of u such that the ground state has no static distortion ($u = 0$). In region II, $E(u)$ develops a shallow local minimum at finite u , and the ground state has a small half-breathing distortion leading to a dimerized state. We note that the energy well for this state is very shallow, implying that the dimerization fluctuates significantly even at low temperatures. In region III, appearing at large e -ph coupling strength, the total energy $E(u)$ monotonically decreases as u increases, indicating that the lattice is unstable. The boundary for this region is determined by the condition $|gu| > 1$, which corresponds to the boundary where the effective hopping integral changes sign.

Nonadiabatic case. Next, we study a nonadiabatic case at finite temperatures with $\omega_{\text{ph}} = \sqrt{2} \text{ eV}$, $M = 1$, and $L = 16$ unit cells using QMC. (For details of the method, we refer the reader to Refs. [21,52].) We now include the individual atomic motion of each $2p_x$ orbital along the chain direction.

Figure 2(a) plots the displacement correlation function $S_x(d) = \frac{1}{L} \sum_i \langle \hat{x}_{i+d} \hat{x}_i \rangle$ at $T = 580 \text{ K}$. At $g = 0.6$ and $g = 0.7$, the $q = \pi$ correlations are short ranged; for $g = 0.8$, they grow stronger and extend across the entire cluster. In the latter case, the error bars are larger than the mean value, indicating that the lattice displacements fluctuate significantly at this temperature. Figure 2(b) shows the variation of $g^2 \langle \hat{x}^2 \rangle$ as a function of g . This quantity increases with coupling when $g \leq 0.8$ but rapidly jumps above one when $g > 0.8$, implying that the lattice is unstable for these larger couplings. Note, the results for $g > 0.8$ are obtained at $T = 1160 \text{ K}$ because the average fermion sign for $g = 0.9$ and $T = 580 \text{ K}$ is extremely small [see Fig. 2(c)]. Based on these results,

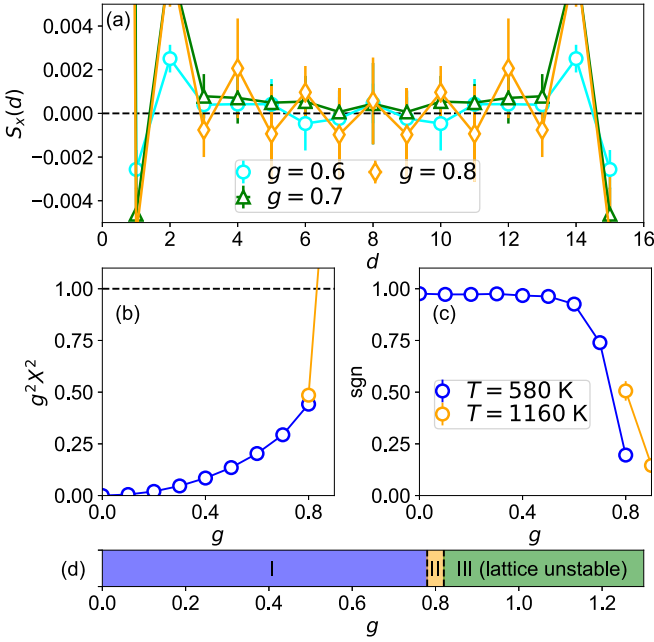


FIG. 2. (a) The displacement correlation function $\langle S_x(d) \rangle$ for three different values of g at $T = 580$ K. (b) The variation of $g^2 X^2$ as a function of the e -ph coupling strength g . (c) The average value of the sign as a function of g . (d) A sketch of the pseudo phase diagram as a function of g .

it is difficult to determine whether the strong fluctuations at $g = 0.8$ will give way to a long-range ordered state at a lower temperature. Nevertheless, we can qualitatively divide the parameter space into three regions, shown in Fig. 2(d). In region I ($g < 0.78$), the system has strong antiferromagnetic correlations and short-range dimerization fluctuations; in region II ($0.78 < g < 0.82$), the system has antiferromagnetic (see Figs. 3 and 4) and dimerization fluctuations; finally, in region III ($g > 0.82$), the system is unstable. We also observe region III in our ED studies using quantum phonons (see Supplemental Material [55]).

Finite-temperature magnetic correlations. Our primary goal is to study the effect of the SSH-like e -ph interaction on the magnetic properties in the cuprates. To address this question, we trace the evolution of the uniform magnetic and dynamical spin susceptibility as a function of g . Figure 3(a) plots the density of states (DOS) at the Fermi level $D(\omega = 0)$ as a function of temperature. For $g = 0$, $D(0)$ approaches zero around $T \approx 967$ K, indicative of a metal-to-insulator transition. The inset of Fig. 3(a) shows the DOS over a wider energy interval at $T = 725$ K, which also exhibits a clear gap at $\omega = 0$. When $g \neq 0$, the metal-to-insulator transition shifts to lower temperatures, and the corresponding Mott gap narrows.

To gain insight into the effect of bond-stretching phonons on the magnetic properties, we calculate the uniform magnetic susceptibility $\chi_m(q = 0) = \beta \sum_i \langle \hat{S}_i^z \hat{S}_0^z \rangle$. Here, $\hat{S}_i^z = \sum_\gamma \hat{S}_{i,\gamma}^z$ is the total spin operator for the unit cell [52]. For a spin-1/2 system such as Sr_2CuO_3 , the uniform magnetic susceptibility is frequently used by experimentalists to determine the value of the effective superexchange coupling J [56–59]. We apply the same methodology here. Figure 3(b) plots χ_m vs T for

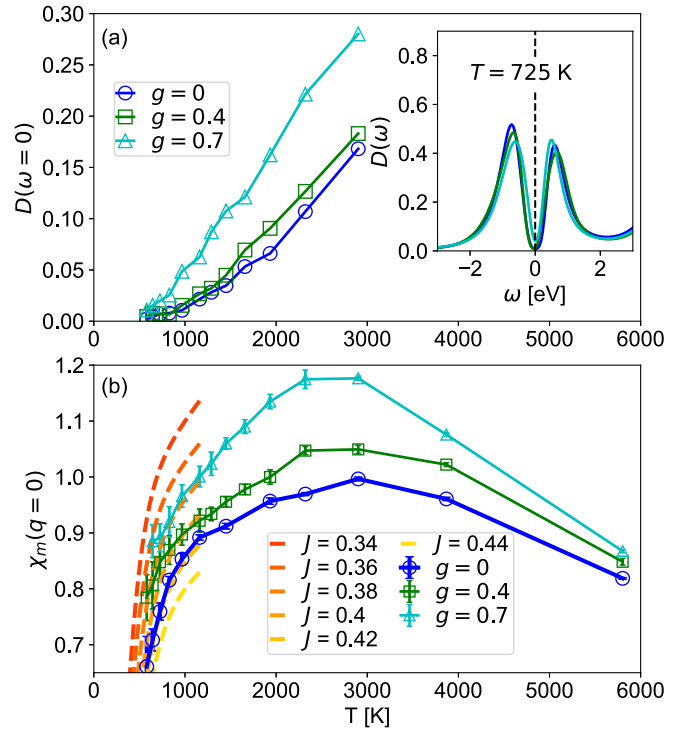


FIG. 3. (a) The density of states $D(\omega)$ as a function of temperature for three different e -ph coupling strengths g . The inset plots the density of states in the frequency space at $T = 725$ K. (b) The uniform magnetic susceptibility $\chi_m(q = 0)$ as a function of temperature. The dashed curves show the results of the Heisenberg model.

several values of g . For comparison, the dashed curves represent results obtained from exactly diagonalizing a Heisenberg model defined on an $L = 16$ site chain with different values of J . For $g = 0$, the low-temperature behavior of χ_m overlaps with Heisenberg model predictions when $J = 0.42$ eV. This observation implies that a simple Heisenberg model can capture the magnetic behavior of the multi-orbital system for our choice of parameters. Increasing the e -ph interaction increases χ_m of the pd model, implying that the effective superexchange interaction is suppressed. We also find that the pd model's χ_m for $g = 0.4$ and $g = 0.7$ deviate from predictions of the Heisenberg model at low temperatures. This discrepancy likely originates from the increased role of the oxygen atoms at these coupling strengths.

The suppression of the superexchange interaction with increasing g can be rationalized using a mean-field analysis. At half filling, J can be obtained using perturbation theory and is given by $J = \frac{t_{pd,1}^2 t_{pd,2}^2}{\Delta_{dp}^2} \left(\frac{1}{\Delta_{dp} + U_p/2} + \frac{1}{U_d} \right)$ [60,61]. Here, $\Delta_{dp} = \epsilon_d - \epsilon_{p_x}$, and $t_{pd,1/2}$ is the hopping integral between $2p_x$ and the left/right $3d_{x^2-y^2}$ orbitals. When the oxygen atom moves away from its equilibrium position, J becomes $J(1 - g^2 x^2)^2$. Consequently, the SSH interaction suppresses the effective superexchange interaction. While this analysis neglects potential phonon-induced renormalization of the Hubbard interaction, it does demonstrate that the modulation of hopping integrals induced by the lattice displacement suppresses the effective superexchange interaction.

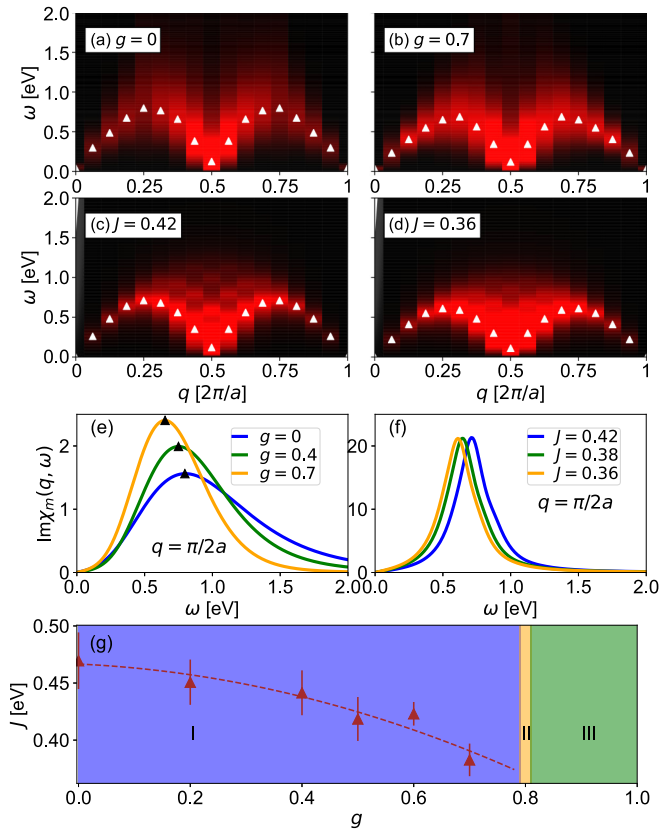


FIG. 4. The imaginary part of the dynamical magnetic susceptibility $\text{Im } \chi_m(q, \omega)$ at $T = 645$ K. (a) and (b) show DQMC results for $\text{Im } \chi_m(q, \omega)$ of the pd model with an e -ph coupling strength $g = 0$ and 0.7 , respectively. (c) and (d) show ED results for $\text{Im } \chi_m(q, \omega)$ of the Heisenberg model for $J = 0.42$ and 0.36 , respectively. (e) and (f) plot $\text{Im } \chi_m(q, \omega)$ at $q = \frac{\pi}{2a}$ for the pd and Heisenberg models, respectively. (g) plots the estimated effective superexchange interaction of the pd model as a function of the e -ph coupling strength.

Next, we analyze the imaginary part of the dynamical magnetic susceptibility $\text{Im } \chi_m(q, \omega)$, which is plotted in Fig. 4. Here, Figs. 4(a) and 4(b) present DQMC results of the pd model, while Figs. 4(c) and 4(d) show ED results of the 1D Heisenberg model. The white triangles denote the frequency $\omega_m(q)$ of the maximum of the spectra at each momentum point. Our system is a charge-transfer insulator with robust antiferromagnetic correlations at low temperatures and half filling. Its low-energy magnetic excitations are therefore characterized by a two-spinon continuum [62,63], which is observed in both the pd and Heisenberg model results. Compared to the results at $g = 0$, $\omega_m(q)$ of the pd model is smaller at $g = 0.7$. For better visualization, Fig. 4(e) plots $\text{Im } \chi_m(q, \omega)$ for $g = 0, 0.4$, and 0.7 at $q = \frac{\pi}{2a}$. Here, we observe that the peak in the susceptibility softens to lower energy and spectral weight is concentrated at lower energies as g increases. Figure 4(f) shows that an effective Heisenberg model would capture the softening but does not capture the redistribution of the spectral weight. This inconsistency occurs because the effective Heisenberg model cannot correctly describe the distribution of the local moment onto the oxygen sites [52], which will also be modulated by the SSH modes.

As an alternative to fitting the uniform magnetic susceptibility, we can estimate the effective J by adjusting the interaction in the Heisenberg model to fit $\omega_m(q)$ of the pd model. Figure 4(g) plots the estimated superexchange interaction J extracted from our DQMC simulations as a function of g . At $g = 0$, the superexchange interaction is about 0.46 eV, which is slightly larger than the value shown in Fig. 3(b) ($J = 0.42$ eV). Due to the thermal broadening and the maximum entropy method, the spectra have a broad peak. We, therefore, provide approximate error bars for our fits, which are estimated as the energy range over which $\text{Im } \chi_m(q, \omega) \geq 0.99 \text{Im } \chi_m[q, \omega_m(q)]$. As the e -ph coupling strength increases in region I of our phase diagram, the effective superexchange interaction decreases, consistent with our analysis in Fig. 3.

Summary. We studied the effects of SSH-like e -ph interaction in a four-orbital Hubbard-SSH model for cuprate spin chains. The model only supports a dimerized state in an extremely narrow window of e -ph coupling strengths in the adiabatic limit and at zero temperature. In the nonadiabatic case, the dimerized state is replaced by strong lattice fluctuations at a finite temperature. In both cases, we found that the lattice becomes unstable when the e -ph coupling exceeds a critical value roughly corresponding to the point where the effective hopping changes sign. Our results suggest that achieving a dimerized state in the linear Hubbard-SSH model may be challenging; however, this state could be stabilized by including nonlinear couplings or anharmonic lattice potentials neglected by our model.

We also examined the pd model's electronic and magnetic properties as a function of e -ph coupling strengths. By mapping the pd model's magnetic properties to an effective Heisenberg model, we find that the effective superexchange interaction decreases quadratically with the e -ph coupling strength in the region where the linear SSH interaction is physical. Our results, therefore, speak against the idea that these interactions can enhance AFM correlations in cuprate materials [64]. In addition, we demonstrate that different e -ph interactions can generate opposite effects on the superexchange coupling.

Understanding the hidden role of the oxygen atom on the superexchange interaction is essential to understanding the superconductivity in the cuprates, where the spin fluctuations play a crucial role in the extraordinary electronic properties. Numerical studies of the t - J model demonstrate that the superconducting temperature strongly depends on the superexchange interaction [65]. Our theoretical analysis implies that the SSH-like e -ph interaction suppresses the superconductivity, while the Holstein-like e -ph interaction enhances the superconductivity. It would be interesting to study a model with both e -ph interactions to understand the role of bond-stretching phonons in the cuprates.

Finally, our results may be relevant to other transition metal oxides. For example, a recent experiment on the infinite-layer nickelate PrNiO_2 [66] found that the superexchange interaction is suppressed under the application of 1% compressive strain, while the opposite behavior is observed in La_2CuO_4 [67]. Empirically, J in an insulator is expected to be proportional to the inverse of the interatomic distance and should, therefore, be enhanced by a compressive strain. The suppressed superexchange interaction in PrNiO_2 could be

attributed to the SSH-like e -ph interaction as proposed in our work via an increase in the effective e -ph coupling constant.

Acknowledgments. The authors thank Mona Berciu, Benjamin Cohen-Stead, and Richard Scalettar for their valuable discussions and comments on this work. S.L. was supported by the U.S. Department of Energy, Office of Basic Energy Sciences, Materials Sciences, and Engineering Division. S.J.

was supported by the U.S. Department of Energy, Office of Science, Office of Basic Energy Sciences, under Award No. DE-SC0022311. This research used resources of the Compute and Data Environment for Science (CADES) at the Oak Ridge National Laboratory, which is supported by the Office of Science of the U.S. Department of Energy under Contract No. DE-AC05-00OR22725.

-
- [1] A. Lanzara, P. V. Bogdanov, X. J. Zhou, S. A. Kellar, D. L. Feng, E. D. Lu, T. Yoshida, H. Eisaki, A. Fujimori, K. Kishio, J. I. Shimoyama, T. Noda, S. Uchida, Z. Hussain, and Z. X. Shen, *Nature (London)* **412**, 510 (2001).
- [2] T. Cuk, D. H. Lu, X. J. Zhou, Z.-X. Shen, T. P. Devereaux, and N. Nagaosa, *Phys. Status Solidi B* **242**, 11 (2005).
- [3] S. Johnston, I. M. Vishik, W. S. Lee, F. Schmitt, S. Uchida, K. Fujita, S. Ishida, N. Nagaosa, Z. X. Shen, and T. P. Devereaux, *Phys. Rev. Lett.* **108**, 166404 (2012).
- [4] J. Li, A. Nag, J. Pelliciani, H. Robarts, A. Walters, M. Garcia-Fernandez, H. Eisaki, D. Song, H. Ding, S. Johnston, R. Comin, and K.-J. Zhou, *Proc. Natl. Acad. Sci. USA* **117**, 16219 (2020).
- [5] L. Chaix, G. Ghiringhelli, Y. Y. Peng, M. Hashimoto, B. Moritz, K. Kummer, N. B. Brookes, Y. He, S. Chen, S. Ishida, Y. Yoshida, H. Eisaki, M. Salluzzo, L. Braicovich, Z.-X. Shen, T. P. Devereaux, and W.-S. Lee, *Nat. Phys.* **13**, 952 (2017).
- [6] L. Braicovich, M. Rossi, R. Fumagalli, Y. Peng, Y. Wang, R. Arpaia, D. Betto, G. M. De Luca, D. Di Castro, K. Kummer, M. Moretti Sala, M. Pagetti, G. Balestrino, N. B. Brookes, M. Salluzzo, S. Johnston, J. van den Brink, and G. Ghiringhelli, *Phys. Rev. Res.* **2**, 023231 (2020).
- [7] J. Lee, K. Fujita, K. McElroy, J. A. Slezak, M. Wang, Y. Aiura, H. Bando, M. Ishikado, T. Masui, J. X. Zhu, A. V. Balatsky, H. Eisaki, S. Uchida, and J. C. Davis, *Nature (London)* **442**, 546 (2006).
- [8] J. Q. Lin, H. Miao, D. G. Mazzone, G. D. Gu, A. Nag, A. C. Walters, M. García-Fernández, A. Barbour, J. Pelliciani, I. Jarrige, M. Oda, K. Kurosawa, N. Momono, K.-J. Zhou, V. Bisogni, X. Liu, and M. P. M. Dean, *Phys. Rev. Lett.* **124**, 207005 (2020).
- [9] C. C. Tam, M. Zhu, J. Ayres, K. Kummer, F. Yakhov-Harris, J. R. Cooper, A. Carrington, and S. M. Hayden, *Nat. Commun.* **13**, 570 (2022).
- [10] R. Hentrich, A. U. B. Wolter, X. Zotos, W. Brenig, D. Nowak, A. Isaeva, T. Doert, A. Banerjee, P. Lampen-Kelley, D. G. Mandrus, S. E. Nagler, J. Sears, Y.-J. Kim, B. Büchner, and C. Hess, *Phys. Rev. Lett.* **120**, 117204 (2018).
- [11] X. Hong, M. Gillig, R. Hentrich, W. Yao, V. Kocsis, A. R. Witte, T. Schreiner, D. Baumann, N. Pérez, A. U. B. Wolter, Y. Li, B. Büchner, and C. Hess, *Phys. Rev. B* **104**, 144426 (2021).
- [12] S. Mu, K. D. Dixit, W. Xiaoping, D. L. Abernathy, H. Cao, S. E. Nagler, J. Yan, P. Lampen-Kelley, D. Mandrus, C. A. Polanco, L. Liang, G. B. Halász, Y. Cheng, A. Banerjee, and T. Berlijn, *Phys. Rev. Res.* **4**, 013067 (2022).
- [13] S. Li and S. Okamoto, *Phys. Rev. B* **106**, 024413 (2022).
- [14] R. Haumont, J. Kreisler, P. Bouvier, and F. Hippert, *Phys. Rev. B* **73**, 132101 (2006).
- [15] D. Bansal, J. L. Niedziela, R. Sinclair, V. O. Garlea, D. L. Abernathy, S. Chi, Y. Ren, H. Zhou, and O. Delaire, *Nat. Commun.* **9**, 15 (2018).
- [16] B. Poojitha, K. Rubi, S. Sarkar, R. Mahendiran, T. Venkatesan, and S. Saha, *Phys. Rev. Mater.* **3**, 024412 (2019).
- [17] W. P. Su, J. R. Schrieffer, and A. J. Heeger, *Phys. Rev. Lett.* **42**, 1698 (1979).
- [18] A. J. Heeger, S. Kivelson, J. R. Schrieffer, and W. P. Su, *Rev. Mod. Phys.* **60**, 781 (1988).
- [19] S. Tang and J. E. Hirsch, *Phys. Rev. B* **37**, 9546 (1988).
- [20] P. Sengupta, A. W. Sandvik, and D. K. Campbell, *Phys. Rev. B* **67**, 245103 (2003).
- [21] S. Li and S. Johnston, *npj Quantum Mater.* **5**, 40 (2020).
- [22] Y. Ohta, T. Tohyama, and S. Maekawa, *Phys. Rev. B* **43**, 2968 (1991).
- [23] S. Johnston, F. Vernay, B. Moritz, Z.-X. Shen, N. Nagaosa, J. Zaanen, and T. P. Devereaux, *Phys. Rev. B* **82**, 064513 (2010).
- [24] E. Berger, P. Valášek, and W. von der Linden, *Phys. Rev. B* **52**, 4806 (1995).
- [25] H. Matsueda, T. Tohyama, and S. Maekawa, *Phys. Rev. B* **74**, 241103(R) (2006).
- [26] E. Khatami, A. Macridin, and M. Jarrell, *Phys. Rev. B* **78**, 060502(R) (2008).
- [27] E. A. Nowadnick, S. Johnston, B. Moritz, R. T. Scalettar, and T. P. Devereaux, *Phys. Rev. Lett.* **109**, 246404 (2012).
- [28] Y. Murakami, P. Werner, N. Tsuji, and H. Aoki, *Phys. Rev. B* **88**, 125126 (2013).
- [29] M. Hohenadler and F. F. Assaad, *Phys. Rev. B* **87**, 075149 (2013).
- [30] A. Nocera, M. Soltanieh-ha, C. A. Perroni, V. Cataudella, and A. E. Feiguin, *Phys. Rev. B* **90**, 195134 (2014).
- [31] E. A. Nowadnick, S. Johnston, B. Moritz, and T. P. Devereaux, *Phys. Rev. B* **91**, 165127 (2015).
- [32] T. Ohgoe and M. Imada, *Phys. Rev. Lett.* **119**, 197001 (2017).
- [33] C. B. Mendl, E. A. Nowadnick, E. W. Huang, S. Johnston, B. Moritz, and T. P. Devereaux, *Phys. Rev. B* **96**, 205141 (2017).
- [34] S. Li, Y. Tang, T. A. Maier, and S. Johnston, *Phys. Rev. B* **97**, 195116 (2018).
- [35] M. Weber and M. Hohenadler, *Phys. Rev. B* **98**, 085405 (2018).
- [36] F. Hébert, B. Xiao, V. G. Rousseau, R. T. Scalettar, and G. G. Batrouni, *Phys. Rev. B* **99**, 075108 (2019).
- [37] Z. Han, S. A. Kivelson, and H. Yao, *Phys. Rev. Lett.* **125**, 167001 (2020).
- [38] N. C. Costa, K. Seki, S. Yunoki, and S. Sorella, *Commun. Phys.* **3**, 80 (2020).
- [39] N. C. Costa, K. Seki, and S. Sorella, *Phys. Rev. Lett.* **126**, 107205 (2021).

- [40] S. Karakuzu, A. Tanjaroon Ly, P. Mai, J. Neuhaus, T. A. Maier, and S. Johnston, *Commun. Phys.* **5**, 311 (2022).
- [41] C. Feng, B. Xing, D. Poletti, R. Scalettar, and G. Batrouni, *Phys. Rev. B* **106**, L081114 (2022).
- [42] B.-T. Ye, L.-Z. Mu, and H. Fan, *Phys. Rev. B* **94**, 165167 (2016).
- [43] B. Xing, W.-T. Chiu, D. Poletti, R. T. Scalettar, and G. Batrouni, *Phys. Rev. Lett.* **126**, 017601 (2021).
- [44] J. Sous, M. Chakraborty, R. V. Krems, and M. Berciu, *Phys. Rev. Lett.* **121**, 247001 (2018).
- [45] A. Nocera, J. Sous, A. E. Feiguin, and M. Berciu, *Phys. Rev. B* **104**, L201109 (2021).
- [46] Q.-G. Yang, D. Wang, and Q.-H. Wang, *Phys. Rev. B* **106**, 245136 (2022).
- [47] H.-X. Wang, Y.-F. Jiang, and H. Yao, [arXiv:2211.09143](https://arxiv.org/abs/2211.09143).
- [48] D. Banerjee, J. Thomas, A. Nocera, and S. Johnston, *Phys. Rev. B* **107**, 235113 (2023).
- [49] Z. Chen, Y. Wang, S. N. Rebec, T. Jia, M. Hashimoto, D. Lu, B. Moritz, R. G. Moore, T. P. Devereaux, and Z.-X. Shen, *Science* **373**, 1235 (2021).
- [50] Y. Wang, Z. Chen, T. Shi, B. Moritz, Z.-X. Shen, and T. P. Devereaux, *Phys. Rev. Lett.* **127**, 197003 (2021).
- [51] V. I. Iglovikov, E. Khatami, and R. T. Scalettar, *Phys. Rev. B* **92**, 045110 (2015).
- [52] S. Li, A. Nocera, U. Kumar, and S. Johnston, *Commun. Phys.* **4**, 217 (2021).
- [53] Y. F. Kung, C.-C. Chen, Y. Wang, E. W. Huang, E. A. Nowadnick, B. Moritz, R. T. Scalettar, S. Johnston, and T. P. Devereaux, *Phys. Rev. B* **93**, 155166 (2016).
- [54] N. A. Bogdanov, G. L. Manni, S. Sharma, O. Gunnarsson, and A. Alavi, *Nat. Phys.* **18**, 190 (2022).
- [55] See Supplemental Material at <http://link.aps.org/supplemental/10.1103/PhysRevB.108.L201113> for more results.
- [56] J. C. Bonner and M. E. Fisher, *Phys. Rev.* **135**, A640 (1964).
- [57] R. B. Griffiths, *Phys. Rev.* **133**, A768 (1964).
- [58] S. Eggert, I. Affleck, and M. Takahashi, *Phys. Rev. Lett.* **73**, 332 (1994).
- [59] N. Motoyama, H. Eisaki, and S. Uchida, *Phys. Rev. Lett.* **76**, 3212 (1996).
- [60] W. Eskes, G. Sawatzky, and L. Feiner, *Physica C: Superconductivity* **160**, 424 (1989).
- [61] W. Hanke, M. Kiesel, M. Aichhorn, S. Brehm, and E. Arrigoni, *Eur. Phys. J.: Spec. Top.* **188**, 15 (2010).
- [62] M. Karbach, G. Müller, A. H. Bougourzi, A. Fledderjohann, and K.-H. Mütter, *Phys. Rev. B* **55**, 12510 (1997).
- [63] J.-S. Caux and R. Hagemans, *J. Stat. Mech.: Theory Exp.* (2006) P12013.
- [64] X. Cai, Z.-X. Li, and H. Yao, *Phys. Rev. Lett.* **127**, 247203 (2021).
- [65] E. Dagotto, *Rev. Mod. Phys.* **66**, 763 (1994).
- [66] Q. Gao, S. Fan, Q. Wang, J. Li, X. Ren, I. Biao, A. Drewanowski, P. Rothenbühler, J. Choi, Y. Wang, T. Xiang, J. Hu, K.-J. Zhou, V. Bisogni, R. Comin, J. Chang, J. Pellicciari, X. J. Zhou, and Z. Zhu, [arXiv:2208.05614](https://arxiv.org/abs/2208.05614).
- [67] O. Ivashko, M. Horio, W. Wan, N. B. Christensen, D. E. McNally, E. Paris, Y. Tseng, N. E. Shaik, H. M. Rønnow, H. I. Wei, C. Adamo, C. Lichtensteiger, M. Gibert, M. R. Beasley, K. M. Shen, J. M. Tomczak, T. Schmitt, and J. Chang, *Nat. Commun.* **10**, 786 (2019).